

We thank the editor for carefully reading our manuscript and for the feedback aimed at helping us to further improve the manuscript.

### **Comments to the Author:**

*Dear authors,*

*Please integrate your arguments from the rebuttal into the manuscript to avoid misinterpretations:*

*- connection to Aquavit campaign*

=> We added some sentences for clarification

*- reference to other instruments from same group if applicable*

=> We reviewed the references and the description of the instrument family

*- (possible) application of SEALDH-II for UTLS measurements*

=> We added information in conclusion and outlook

*- use of the terms "new" and "holistic"*

=> We revised and explained these terms in the paper.

*Potential unclear issues spotted by the editor:*

*- mixing ratio vs. mole fraction*

=> We clarified that in the paper

*- use of "mid" and "upper" atmosphere*

=> We clarified that in the paper

# Absolute, pressure dependent validation of a calibration-free, airborne laser hygrometer transfer standard (SEALDH-II) from 5 – 1200 ppmv using a metrological humidity generator

Bernhard Buchholz<sup>1,2,4</sup>, Volker Ebert<sup>1,2,3</sup>

<sup>1</sup> Physikalisch-Technische Bundesanstalt Braunschweig, Germany

<sup>2</sup> Physikalisch Chemisches Institut, Universität Heidelberg, Germany

<sup>3</sup> Center of Smart Interfaces, Technische Universität Darmstadt, Germany

<sup>4</sup> currently at Department of Civil and Environmental Engineering, Princeton University, USA

Corresponding author: volker.ebert@ptb.de

**Gelöscht:** Absolute, pressure dependent validation of a calibration-free, airborne laser hygrometer transfer standard (SEALDH-II) from 5 – 1200 ppmv using a metrological humidity generator ¶

**Gelöscht:** SEALDH-II – a calibration-free transfer standard for airborne water vapor measurements: Pressure dependent absolute validation from 5 – 1200 ppmv . at a metrological humidity generator ¶

## Abstract

Highly accurate water vapor measurements are indispensable for understanding a variety of scientific questions as well as industrial processes. While in metrology water vapor concentrations can be defined, generated and measured with relative uncertainties in the single percentage range, field deployable airborne instruments deviate even under quasi-static laboratory conditions up to 10-20%. The novel SEALDH-II hygrometer, a calibration-free, tuneable diode laser spectrometer, bridges this gap by implementing a new holistic concept to achieve higher accuracy levels in the field. Here we present the absolute validation of SEALDH-II at a traceable humidity generator during 23 days of permanent operation at 15 different H<sub>2</sub>O concentration levels between 5 and 1200 ppmv. At each concentration level, we studied the pressure dependence at 6 different gas pressures between 65 and 950 hPa. Further, we describe the setup for this metrological validation, the challenges to overcome when assessing water vapor measurements on a high accuracy level, as well as the comparison results. With this validation, SEALDH-II is the first airborne, metrologically validated humidity transfer standard which links several scientific airborne and laboratory measurement campaigns to the international metrological water vapor scale.

## 1. Introduction

Water vapor affects, like no other substance, nearly all atmospheric processes (Ludlam, 1980; Möller et al., 2011; Ravishankara, 2012). Water vapor represents not only a large direct feedback to global warming when forming clouds, but also plays a major role in atmospheric chemistry (Held and Soden, 2000; Houghton, 2009; Kiehl and Trenberth, 1997). Changes in the water distribution, as vapor or in condensed phases (e.g. in clouds), have a large impact on the radiation balance of the atmosphere. This justifies that water vapor is often mentioned as the most important greenhouse gas and one of the most important parameters in climate research (Ludlam, 1980; Maycock et al., 2011). Water vapor measurements are often needed for other in-situ atmospheric analyzers to correct for their water vapor cross-interference. The high (spatial and

temporal) variability of atmospheric water vapor, its large dynamic range (typically 3 – 40 000 ppmv<sup>1</sup>), and its broad spectroscopic fingerprint typically require complex multi-dimensional calibrations, in particular for spectroscopic sensors. These calibrations often embrace the water vapor content of the gas flow to be analyzed as one of the key calibration parameters even if the instrument (e.g. for CO<sub>2</sub>), is not intended to measure water vapor at all.

In particular for field weather stations, water vapor analyzers often are seen as part of the standard instrumentation in atmospheric research. This seems reasonable due to several reasons: slow H<sub>2</sub>O concentration change over hours, the typical mid-range humidity levels (approx. above 5000 ppmv), no significant gas pressure or temperature change, target accuracy often only in the on the order of 5-15% relative deviation, and the absence of “non-typical atmospheric components” such as soot or hydrophobic substances. Water vapor measurements under these conditions can be performed by a variety of different devices (Wiederhold, 1997): Capacitive polymer sensors e.g. (Salasmaa and Kostamo, 1986) are frequently deployed in low cost (field) applications. Small-scale produced, commercially available spectral absorption devices e.g. (Petersen et al., 2010) are often used in research campaigns. Dew-point mirror hygrometers (DPM) are known for their high accuracy. However, this is only true if they are regularly calibrated at high accuracy (transfer-) standards in specialized hygrometry laboratories such as in metrology institutes (Heinonen et al., 2012).

As soon as hygrometers have to be deployed in harsh environments (e.g. on airborne platforms), this situation changes entirely: The ambient gas pressure (10 – 1000 hPa) and gas temperature (-90 – 40°C) ranges are large and both values change rapidly, the required H<sub>2</sub>O measurement range is set by the ambient atmosphere (typically 3 – 40000 ppmv), mechanical stress and vibrations occur, and the sampled air contains additional substances from condensed water (ice, droplets), particles, or even aircraft fuel vapor (e.g. on ground). These and other impacts complicate reliable, accurate, long-term stable H<sub>2</sub>O measurements and briefly outline why water vapor measurements remain difficult in-situ measurements in the field, even if they are nearly always needed in atmospheric science. Usually, the availability and coverage of observations limit model validation studies in the first place but also the lack of sufficient accuracy may have limited important scientific interpretations (Krämer et al., 2009; Peter et al., 2006; Scherer et al., 2008; Sherwood et al., 2014).

Over the last decades, numerous hygrometers were developed and deployed on aircraft (Buck, 1985; Busen and Buck, 1995; Cerni, 1994; Desjardins et al., 1989; Diskin et al., 2002; Durry et al., 2008; Ebert et al., 2000; Gurlit et al., 2005; Hansford et al., 2006; Helten et al., 1998; Hunsmann et al., 2008; Karpechko et al., 2014; Kley and Stone, 1978; May, 1998; Meyer et al., 2015; Ohtaki and Matsui, 1982; Roths and Busen, 1996; Salasmaa and Kostamo, 1986; Schiff et al., 1994; Silver and Hovde, 1994a, 1994b; Thornberry et al., 2014;

Webster et al., 2004; Zöger et al., 1999a, 1999b) (non-exhaustive list). While for some atmospheric questions the quality level of the data often is sufficient (e.g. typically climatologies), there are also a variety of questions, especially validation of atmospheric models, where the required absolute accuracy, precision,

Gelöscht:

Gelöscht: ),

Gelöscht: but those often show results which are not sufficient for

Gelöscht: in terms of the

<sup>1</sup> SEALDH-II native unit for H<sub>2</sub>O concentration measurement is mole fraction. The SI conform unit would be mol/mol. We kept the ppmv (= μmol/mol) since most atmospheric communities are more used to it.

temporal resolution, long-term stability, comparability, etc. needs to be higher. These problems can be grouped into two major categories: accuracy linked problems and time response linked problems. The latter is particularly important for investigations in heterogeneous regions in the lower troposphere as well as for investigations in clouds. In these regions, even two on average agreeing instruments with different response times yield local, large, relative deviations on the order of up to 30% (Smit et al., 2014). It is important to keep in mind, that the total time response of a system is a superposition of the time response components of the instrument itself as well as of the sampling inlet. These typically depend on numerous parameters like e.g. type of inlet, inlet pipe length, pipe coding, pipe temperature, pipe heating, gas flow, input air humidity level, etc.

In contrast to time response studies, accuracy linked problems in flight are difficult to isolate since they are always covered by the spatial variability (which leads to temporal variability for moving aircraft) of atmospheric H<sub>2</sub>O distribution. Comparing hygrometer in flight, such as, for example in (Rollins et al., 2014), does not facilitate a clear accuracy assessment.

Therefore in 2007, an international intercomparison exercise named “AquaVIT” (Fahey et al., 2014) was carried out to compare airborne hygrometers under quasi-static, laboratory-like conditions for upper tropospheric and lower stratospheric humidity levels. AquaVIT (Fahey et al., 2014) encompassed 22 instruments from 17 international research groups. The instruments were categorized in well-validated, often deployed “core” instruments (APiC, FISH, FLASH, HWV, JLH, CFH) and “younger” non-core instruments. AquaVIT revealed in the important 1 to 150 ppmv H<sub>2</sub>O range, that -even under quasi-static conditions- the deviation between the core instrument’s readings and their averaged group mean was on the order of  $\pm 10$  %. This result fits to the typical interpretation problems of flight data where instruments often deviate from each other by up to 10%, which is not covered by the respective uncertainties of the individual instruments. AquaVIT was a unique first step to document and improve the accuracy of airborne measurements in order to make them more comparable. However, no instrument could claim after AquaVIT that its accuracy is higher than any other AquaVIT instrument, since no “gold standard” was part of the campaign, i.e., a metrological transfer standard (JCGM 2008, 2008; Joint Committee for Guides in Metrology (JCGM), 2009) traced back to the SI units. There is no physical argument for the average being better than the measured value of a single instrument. Instead, many arguments speak for systematic deviations of airborne hygrometers: Most hygrometers have to be calibrated. Even for a perfect instrument, the accuracy issue is represented by the calibration source and its gas handling system, which in this case leads to two major concerns: First, one has to guarantee that the calibration source is accurate and stable under field conditions, i.e., when using it before or after a flight on the ground. This can be challenging especially for the transportation of the source with all its sensitive electronics/mechanics and for the deviating ambient operation temperature from the ambient validation temperature (hangar vs. laboratory). Even more prone to deviations are calibration sources installed inside the aircraft due to changing ambient conditions such as cabin temperature, cabin pressure, orientation angle of instrument (important, if liquids are used for heating or cooling). Secondly, the gas stream with a highly defined amount of water vapor has to be conveyed into the instrument. Especially for water vapor, which is a strongly polar molecule, this gas

- Gelöscht: i
- Gelöscht: I
- Gelöscht: is
- Gelöscht: 's time response plus
- Gelöscht: system's time response which
- Gelöscht: s
- Gelöscht: many
- Gelöscht: (
- Gelöscht: (
- Gelöscht: ed?
- Gelöscht: )
- Gelöscht: )
- Gelöscht:

142 transport can become a critical step. Changing from high to low concentrations or even just changing the  
 143 gas pressure or pipe temperature can lead to signal creep due to slow adsorption and desorption processes,  
 144 which can take long to equilibrate. In metrology, this issue is solved by a long validation/calibration time  
 145 (hours up to weeks, depending on the H<sub>2</sub>O concentration level), a generator without any connectors/fittings  
 146 (everything is welded) and piping made out of electro-polished, stainless steel to ensure that the  
 147 equilibrium is established before the actual calibration process is started. However, this calibration  
 148 approach is difficult to deploy and maintain for aircraft/field operations due to the strong atmospheric  
 149 variations in gas pressure and H<sub>2</sub>O concentrations, which usually leads to a multi-dimensional calibration  
 150 pattern (H<sub>2</sub>O concentration, gas pressure, sometimes also gas temperature) in a short amount of calibration  
 151 time (hours). Highly sensitive, frequently flown hygrometers like (Zöger et al., 1999a) are by their physical  
 152 principle, not as long-term stable as it would be necessary to take advantage of a long calibration session.  
 153 Besides the time issue to reach a H<sub>2</sub>O equilibrium between source and instrument, most calibration  
 154 principles for water vapor are influenced by further issues. A prominent example is the saturation of air in  
 155 dilution/saturation based water vapor generators: gas temperature and pressure defines the saturation level  
 156 (described e.g. by Sonntag's Equation (Rollins et al., 2014)), however, it is well-known that e.g. 100.0%  
 157 saturation is not easily achievable. This might be one of the impact factors for a systematic offset during  
 158 calibrations in the field. The metrology community solves this for high humidity levels with large, multi-  
 159 step saturation chambers which decrease the temperature step-wise to force the water vapor to condense in  
 160 every following step. These few examples of typical field-related problems show, that there is a reasonable  
 161 doubt that deviations in field situations are norm-distributed. Hence, the mean during AquaVIT might be  
 162 biased, i.e. not the correct H<sub>2</sub>O value.

163 The instruments by themselves might actually be more accurate than AquaVIT showed, but deficiencies of  
 164 the different calibration procedures (with their different calibration sources etc.) might mask this. To  
 165 summarize, AquaVIT documented a span of up to 20% relative deviation between the world's best airborne  
 166 hygrometers – but AquaVIT could not assess absolute deviations nor explain them, since a link to a

167 metrological H<sub>2</sub>O primary standard (i.e., the definition of the international water vapor scale) was missing.  
 168 While AquaVIT focused primarily on the stratospheric H<sub>2</sub>O range from 0 – 150 ppmv) whereas SEALDH-II  
 169 is a wide-range instrument(3 – 40000 ppmv),it is nevertheless evident that the large overlap region (from 5  
 170 to 150 ppmv) between our validation, AquaVIT's, and SEALDH-II's concentration range will allow to infer  
 171 new and sustainable statements from our validation results.

172 Therefore, we present in this paper the first comparison of an airborne hygrometer (SEALDH-II) with a  
 173 metrological standard for the atmospheric relevant gas pressure (65 – 950 hPa) and H<sub>2</sub>O concentration  
 174 range (5 – 1200 ppmv). We will discuss the validation setup, procedure, and results. Based on this  
 175 validation, SEALDH-II is by definition the first airborne transfer standard for water vapor which links  
 176 laboratory and field campaigns directly to metrological standards.

177

Gelöscht: Even though,

Gelöscht: (

Gelöscht: while

Gelöscht: beeingbeing

Gelöscht: (3 – 40000 ppmv)

Gelöscht: the

Gelöscht: of

Gelöscht: –

Gelöscht: our

Gelöscht: allow to infer

Gelöscht: infer

Gelöscht: ring from the validations  
results

Gelöscht: s

## 192 2. SEALDH-II

### 193 2.1. System description

194 This paper focuses on the metrological accuracy validation of the Selective Extractive Airborne Laser Diode  
195 Hygrometer (SEALDH-II). SEALDH-II is the airborne successor of the proof-of-concept spectrometer  
196 (SEALDH-I) study published in (Buchholz et al., 2014), which showed the possibility and the achievable  
197 accuracy level for calibration-free dTDLAS hygrometry. The publication (Buchholz et al., 2014)  
198 demonstrates this for the 600 ppmv to 20000 ppmv range at standard ambient pressure. The instruments

Gelöscht: )

199 SEALDH-I, SEALDH-II and also HAI (Buchholz et al., 2017) are all three built with the design philosophy  
200 that every single reported value of the instrument should have a “related boundary/operation condition  
201 snap shot” allowing to exclude the possibility of any instrumental malfunction during the measurement.

Gelöscht: “holistic”

202 SEALDH-II is from this perspective the most extensive approach (capturing much more boundary  
203 condition data (Buchholz et al., 2016)), while HAI can serve as a multi-channel, multi-phase hygrometer for  
204 a broader variety of scientific questions.

205 SEALDH-II integrates numerous different principles, concepts, modules, and novel parts, which contribute  
206 to or enable the results shown in this paper. SEALDH-II is described in detail in (Buchholz et al., 2016). The  
207 following brief description covers the most important technical aspects of the instrument from a user’s  
208 point of view:

Gelöscht: SEALDH-II’s high internal complexity does not allow a full, detailed discussion of the entire instrument in this paper;

Gelöscht: for more details the reader is referred to

209 SEALDH-II is a compact (19” rack 4 U (=17.8 cm)) closed-path, absolute, directly Tunable Diode Laser  
210 Absorption Spectroscopy (dTDLAS) hygrometer operating at 1.37  $\mu\text{m}$ . With its compact dimensions and the  
211 moderate weight (24 kg), it is well suited for space- and weight-limited airborne applications. The internal  
212 optical measurement cell is a miniaturized White-type cell with an optical path length of 1.5 m (Kühnreich  
213 et al., 2016; White, 1976). It is connected to the airplane’s gas inlet via an internal gas handling system  
214 comprising a temperature exchanger, multiple temperature sensors, a flow regulator, and two gas pressure  
215 sensors.

216 Approximately 80 different instrument parameters are controlled, measured, or corrected by SEALDH-II at  
217 any time to provide an almost complete supervision and detection of the spectrometer status – we termed  
218 this concept “holistic dTDLAS spectroscopy” (Buchholz and Ebert, 2014a). This extensive set of monitoring  
219 data ensures reliable and well-characterized measurement data at any time. The knowledge about the  
220 instruments status strongly facilitates metrological uncertainties calculations. SEALDH-II’s calculated linear  
221 part of the measurement uncertainty is 4.3%, with an additional offset uncertainty of  $\pm 3$  ppmv (further

Gelöscht: holistic wide-ranging view

Gelöscht: on

Gelöscht: .

Gelöscht:

222 details in (Buchholz et al., 2016)). The precision of SEALDH-II was determined via the Allan-variance  
223 approach and yielded 0.19 ppmv (0.17 ppmv·m·Hz<sup>-1/2</sup>) at 7 Hz repetition rate and an ideal precision of 0.056  
224 ppmv (0.125 ppmv·m·Hz<sup>-1/2</sup>) at 0.4 Hz. In general, SEALDH-II’s time response is limited by the gas flow  
225 through the White-type multi-pass measurement cell with a volume of 300 ml. With the assumption of a  
226 bulk flow of 7 SLM at 200 hPa through the cell, the gas exchange time is 0.5 seconds.

SEALDH-II's measurement range covers 3 – 40000 ppmv. The calculated mixture fraction offset uncertainty of  $\pm 3$  ppmv defines the lower detection limit. This offset uncertainty by itself is entirely driven by the capability of detecting and minimizing parasitic water vapor absorption. The concept, working principle, and its limits are described in (Buchholz and Ebert, 2014b). The upper limit of 40000 ppmv is defined by the lowest internal instrument temperature, which has to always be higher than the dew point temperature to avoid any internal condensation. From a spectroscopic perspective, SEALDH-II could handle concentrations up to approx. 100000 ppmv before spectroscopic problems like saturation limit the accuracy and increase the relative uncertainty beyond 4.3%.

## 2.1. Calibration-free evaluation approach

SEALDH-II's data treatment works differently from nearly all other published TDLAS spectrometers. Typically, instruments are setup in a way that they measure the absorbance or a derivative measurand of absorbance, and link it to the H<sub>2</sub>O concentration. This correlation together with a few assumptions about long-term stability, cross interference, gas temperature dependence, gas pressure dependence is enough to calibrate a system (Muecke et al., 1994). Contrarily, a calibration-free approach requires a fully featured physical model describing the absorption process entirely. The following description is a brief overview; for more details see e.g. (Buchholz et al., 2014, 2016; Ebert and Wolfrum, 1994; Schulz et al., 2007).

In a very simplified way, our physical absorption model uses the *extended* Lambert-Beer equation (Equation 1) which describes the relationship between the initial light intensity  $I_0(\lambda)$  before the absorption path (typically being in the few mW-range) and the transmitted light intensity  $I(\lambda)$ .

Equation 1:  $I(\lambda) = E(t) + I_0(\lambda) \cdot Tr(t) \cdot \exp[-S(T) \cdot g(\lambda - \lambda_0) \cdot N \cdot L]$

The parameter  $S(T)$  describes the line strength of the selected molecular transition. In SEALDH-II's case, the spectroscopic multi-line fit takes into account 19 transition lines in the vicinity of the target line at 1370 nm (energy levels: 110 – 211, rotation-vibrational combination band). The other parameters are the line shape function  $g(\lambda - \lambda_0)$ , the absorber number density  $N$ , the optical path length  $L$  and corrections for light-type background radiation  $E(t)$  and broadband transmission losses  $Tr(t)$ .

Equation 1 can be enhanced with the ideal gas law to calculate the H<sub>2</sub>O volume mole fraction  $c$ :

Gelöscht: mixing

Gelöscht: ratio

Equation 2: 
$$c = -\frac{k_B \cdot T}{S(T) \cdot L \cdot p} \int \ln \left( \frac{I(v) - E(t)}{I_0(v) \cdot Tr(t)} \right) \frac{dv}{dt} dt$$

The additional parameters in Equation 2 are: constant entities like the Boltzmann constant  $k_B$ ; the optical path length  $L$ ; molecular constants like the line strength  $S(T)$  of the selected molecular transition; the dynamic laser tuning coefficient  $\frac{dv}{dt}$ , which is a constant laser property; continuously measured entities such as gas pressure ( $p$ ), gas temperature ( $T$ ) and photo detector signal of the transmitted light intensity  $I(v)$  as well as the initial light intensity  $I_0(v)$ , which is retrieved during the evaluation process from the transmitted light intensity  $I(v)$ .

Equation 2 facilitates an evaluation of the measured spectra without any instrument calibration at any kind of water vapor reference (Buchholz et al., 2014; Ebert and Wolfrum, 1994; Schulz et al., 2007) purely based on first principles. Our concept of a fully calibration-free data evaluation approach (this excludes also any referencing of the instrument to a water standard in order to correct for instrument drift, offsets, temperature dependence, pressure dependence, etc.) is crucial for the assessment of the results described in this publication. It should be noted that the term “calibration-free” is frequently used in different communities with dissimilar meanings. We understand this term according to the following quote (JCGM 2008, 2008): “calibration (...) in a first step, establishes a relation between the measured values of a quantity with measurement uncertainties provided by a measurement standard (...), in a second step, [calibration] uses this information to establish a relation for obtaining a measurement result from an indication (of the device to be calibrated)”. Calibration-free in this sense means, that SEALDH-II does not use any information from “calibration-, comparison-, test-, adjustment-” runs with respect to a higher accuracy “water vapor standard” to correct or improve any response function of the instrument. SEALDH-II uses as described in (Buchholz et al., 2016) only spectroscopic parameters and the 80 supplementary parameters as measurement input to calculate the final H<sub>2</sub>O concentration. The fundamental difference between a calibration approach and this stringent concept is that only effects which are part of our physical model are taken into account for the final H<sub>2</sub>O concentration calculation. All other effects like gas pressure or temperature dependencies, which cannot be corrected with a well-defined physical explanation, remain in our final results even if this has the consequence of slightly uncorrected results deviations. This strict philosophy leads to measurements which are very reliable with respect to accuracy, precision and the instrument’s over-all performance. The down-side is a relatively computer-intensive, sophisticated evaluation. As SEALDH-II stores all the raw spectra, one could – if needed for whatever reason – also calibrate the instrument by referencing it to a high accuracy water vapor standard and transfer the better accuracy e.g. of a metrological standard onto the instrument. Every calibration-free instrument can be calibrated since pre-requirements for a calibration are just a subset of the requirements for a calibration-free instrument. However, a calibration can only improve the accuracy for the relatively short time between two calibration-cycles by adding all uncertainty contributions linked to the calibration itself to the system. This is unpleasant or even intolerable for certain applications and backs our decision to develop a calibration-free instrument to enable a first principles, long-term stable, maintenance-free and autonomous hygrometer for field use e.g. at remote sites or aircraft deployments.

### 3. SEALDH-II validation facility

#### 3.1. Setup

Figure 1, right shows the validation setup. As a well-defined and highly stable H<sub>2</sub>O vapor source, we use a commercial Thunder scientific model (TSM) 3900, similar to (Thunder-Scientific, 2016). This source saturates pre-dried air at an elevated gas pressure in an internally ice covered chamber. The gas pressure in

Gelöscht: Figure 1Figure 1



the chamber and the chamber's wall temperature are precisely controlled and highly stable and thus define the absolute water vapor concentration via the Sonntag equation (Sonntag, 1990). After passing through the saturator, the gas expands to a pressure suitable for the subsequent hygrometer. The pressure difference between the saturation chamber pressure and the subsequent step give this principle its name "two pressure generator". The stable H<sub>2</sub>O concentration range of the TSM is 1 – 1300 ppmv for these specific deployment conditions. This generator provides a stable flow of approximately 4 – 5 SLM. Roughly 0.5 SLM are distributed to a frost/dew point hygrometer, D/FPH, (MBW 373 ) (MBW Calibration Ltd., 2010). SEALDH-II is fed with approx. 3.5 SLM, while 0.5 SLM are fed to an outlet. This setup ensures that the dew point mirror hygrometer (DPH)<sup>2</sup> operates close to the ambient pressure, where its metrological primary calibration is valid, and that the gas flow is sufficiently high in any part of the system to avoid recirculation of air. The vacuum pump is used to vary the gas pressure in SEALDH-II's cell with a minimized feedback on the flow through the D/FPH and the TSM. This significantly reduces the time for achieving a stable equilibrium after any gas pressure change in SEALDH-II's chamber. SEALDH-II's internal electronic flow regulator limits the mass flow at higher gas pressures and gradually opens towards lower pressures (vacuum pumps usually convey a constant volume flow i.e., the mass flow is pressure dependent). We termed this entire setup "traceable humidity generator", THG, and will name it as such throughout the text.

### 3.1. Accuracy of THG

The humidity of the gas flow is set by the TSM generator but the absolute H<sub>2</sub>O values are traceably determined with the dew point mirror hygrometer (D/FPH). The D/FPH, with its primary calibration, thus guarantees the absolute accuracy in this setup. The D/FPH is not affected by the pressure changes in SEALDH-II's measurement cell and operates at standard ambient gas pressure and gas temperature where its calibration is most accurate. The D/FPH was calibrated (Figure 2) at the German national standard for mid-range humidity (green, 600 – 8000 ppmv) as well as at the German national standard for low-range humidity (blue, for lower values 0.1 – 500 ppmv). The two national standards work on different principles: The two pressure principle (Buchholz et al., 2014) currently supplies the lower uncertainties (green, "±"-values in Figure 2). Uncertainties are somewhat higher for the coulometric generator (Mackrodt, 2012) in the lower humidity range (blue). The "Δ"-values in Figure 2 show the deviations between the readings of the D/FPH and the "true" values of the national primary standards.

Gelöscht: Figure 2Figure 2

Gelöscht: Figure 2Figure 2

Gelöscht: Figure 2Figure 2

<sup>2</sup> The used dew point mirror hygrometer can measure far below 0°C; therefore, it is a dew point mirror above > 0°C and a frost point mirror as soon as there is ice on the mirror surface. We will use both DPH and D/FPH abbreviations interchangeably.

## 341 4. SEALDH-II validation procedure

### 342 4.1. Mid-term multi-week permanent operation of SEALDH-II

343 One part of the validation was a permanent operation of SEALDH-II over a time scale much longer than the  
344 usual air or ground based scientific campaigns. In this paper, we present data from a permanent 23 day  
345 long (550 operation hours) operation in automatic mode. Despite a very rigorous and extensive monitoring  
346 of SEALDH-II's internal status, no malfunctions of SEALDH-II could be detected. One reason for this are  
347 the extensive internal control and error handling mechanisms introduced in SEALDH-II, which are  
348 mentioned above and described elsewhere (Buchholz et al., 2016). [Figure 3](#) shows an overview of the entire  
349 validation. The multi-week validation exercise comprises 15 different H<sub>2</sub>O concentration levels between 2  
350 and 1200 ppmv. At each concentration level, the gas pressure was varied in six steps (from 65 to 950 hPa)  
351 over a range which is particularly interesting for instruments on airborne platforms operating from  
352 troposphere to lower stratosphere where SEALDH-II's uncertainty ( $4.3\% \pm 3$  ppmv) is suitable. [Figure 3](#)  
353 (top) shows the comparison between SEALDH-II (black line) and the THG setup (red). [Figure 3](#) (bottom)  
354 shows the gas pressure (blue) and the gas temperature (green) in SEALDH-II measurement cell. The gas  
355 temperature increase in the second week was caused by a failure of the laboratory air conditioner that led to  
356 a higher room temperature and thus higher instrument temperature. [Figure 4](#) shows the 200 hPa section of  
357 the validation in Figure 3. To avoid any dynamic effects from time lags, hysteresis of the gas setup, or the  
358 instruments themselves, every measurement at a given concentration/pressure combination lasted at least  
359 60 min. The data from the THG (red) show that there is nearly no feedback of a gas pressure change in  
360 SEALDH-II's measurement cell towards the D/FPH, respectively the entire THG. The bottom subplot in  
361 [Figure 4](#) shows the relative deviation between the THG and SEALDH-II. This deviation is correlated to the  
362 absolute gas pressure level and can be explained by deficiencies of the Voigt lines shape used to fit  
363 SEALDH-II's spectra (Buchholz et al., 2014, 2016). The Voigt profile, a convolution of Gaussian (for  
364 temperature broadening) and Lorentzian (pressure broadening) profiles used for SEALDH-II's evaluation,  
365 does not include effects such as Dicke Narrowing, which become significant at lower gas pressures.  
366 Neglecting these effects cause systematic, but long-term stable and fully predictable deviations from the  
367 reference value in the range from sub percent at atmospheric gas pressures to less than 5 % at the lowest gas  
368 pressures described here. We have chosen not to implement any higher order line shape (HOLS) models as  
369 the spectral reference data needed are not available at sufficient accuracy. Further, HOLS would force us to  
370 increase the number of free fitting parameters, which would destabilize our fitting procedure, and lead to  
371 reduced accuracy/reliability (i.e., higher uncertainty) as well as significantly increased computational  
372 efforts. This is especially important for flight operation where temporal H<sub>2</sub>O fluctuations (spatial  
373 fluctuations result in temporal fluctuations for a moving device) occur with gradients up to 1000 ppmv/s.  
374 These well understood, systematic pressure dependent deviations will be visible in each further result plot  
375 of this paper. The impact and methods of compensation are already discussed in (Buchholz et al., 2014). The  
376 interested reader is referred to this publication for a more detailed analysis and description.

Gelöscht: Figure 3Figure 3

Gelöscht: Figure 3Figure 3

Gelöscht: Figure 3Figure 3

Gelöscht: Figure 4Figure 4

Gelöscht: Figure 4Figure 4

SEALDH-II's primary target areas of operations are harsh field environments. Stability and predictability is to be balanced with potential, extra levels of accuracy which might not be required or reliably achievable for the intended application. Higher order line shape models are therefore deliberately traded for a stable, reliable, and unified fitting process under all atmospheric conditions. This approach leads to systematic, predictable deviations in the typical airborne accessible atmospheric gas pressure range (125 – 900 hPa) of less than 3%. One has to compare these results for assessment to the non-systematic deviations of 20% revealed during the mentioned AquaVIT comparison campaign (Fahey et al., 2014). Hence, for field/airborne purposes, the 3% seems to be fully acceptable – especially in highly H<sub>2</sub>O structured environments.

Gelöscht:

This comparison with AquaVIT should just provide a frame to embed the 3%. The H<sub>2</sub>O concentration range of AquaVIT (0 – 150 ppmv) versus this validation range (5 -1200 ppmv) and the instruments configuration at AquaVIT (mainly (upper) stratospheric hygrometers) versus SEALDH-II as a wide range instrument (3 – 40000 ppmv) do not allow a direct comparison. Sadly, there is no other reliable (representative for the community, externally reviewed, blind submission, etc.) comparison exercise such as AquaVIT for higher concentration ranges.

Gelöscht:

#### 4.1. Assessment of SEALDH-II's mid-term accuracy: Dynamic effects

Besides the pressure dependence discussed above, SEALDH-II's accuracy assessment is exacerbated by the differences in the temporal behavior between the THG's dew/frost point mirror hygrometer (D/FPH) and SEALDH-II: [Figure 5](#), (left) shows an enlarged 45 min. long section of measured comparison data. SEALDH-II (black) shows a fairly large water vapor variation compared to the THG (red). The precision of SEALDH-II (see chapter 2) is 0.056 ppmv at 0.4 Hz (which was validated at a H<sub>2</sub>O concentration of 600 ppmv (Buchholz et al., 2016)) yielding a signal to noise ratio of 10700. Therefore, SEALDH-II can very precisely detect variations in the H<sub>2</sub>O concentration. Contrarily, the working principle of a D/FPH requires an equilibrated ice/dew layer on the mirror. Caused by the inertial thermal adjustment process, the response time of a dew/frost point mirror hygrometer has certain limitations due to this principle (the dew/frost point temperature measurement is eventually used to calculate the final H<sub>2</sub>O concentration), whereas the optical measurement principle of SEALDH-II is only limited by the gas transport, i.e., the flow (exchange rate) through the measurement cell. The effect of those different response times is clearly visible from 06:00 to 06:08 o'clock in [Figure 5](#). The gas pressure of SEALDH-II's measurement cell (blue), which is correlated to the gas pressure in the THG's ice chamber, shows an increase of 7 hPa – caused by the regulation cycle of the THG's generator (internal saturation chamber gas pressure change). The response in the THG frost point measurement (green, red) shows a significant time delay compared to SEALDH-II, which detects changes approx. 20 seconds faster. This signal delay is also clearly visible between 06:32 to 06:40 o'clock, where the water vapor variations detected by SEALDH-II are also visible in the smoothed signals of the THG. [Figure 5](#), right shows such a variation in detail (5 min). The delay between the THG and SEALDH-II is here also approximately 20 seconds. If we assume that SEALDH-II measures (due to its high precision) the true water vapor fluctuations, the relative deviation can be interpreted as overshooting and undershooting

Gelöscht: Figure 5Figure 5

Gelöscht: Figure 5Figure 5

Gelöscht: Figure 5Figure 5

424 of the D/FPH's controlling cycle, which is a commonly known response behavior of slow regulation  
425 feedback loops to fast input signal changes. The different time responses lead to "artificial" noise in the  
426 concentration differences between SEALDH-II and THG. Theoretically, one could characterize this behavior  
427 and then try to correct/shift the data to minimize this artificial noise. However, a D/FPH is fundamentally  
428 insufficient for a dynamic characterization of a fast response hygrometer such as SEALDH-II. Thus, the  
429 better strategy is to keep the entire system as stable as possible and calculate mean values by using the  
430 inherent assumption that under- and overshoots of the DPM affect the mean statically and equally. With  
431 this assumption, the artificial noise can be seen in the first order as Gaussian distributed noise within each  
432 pressure step (Figure 4) of at least 60 min. The error induced by this should be far smaller than the above  
433 discussed uncertainties of the THG (and SEALDH-II).

Gelöscht: Figure 4Figure 4

## 435 5. Results

436 The results of this validation exercise are categorized in three sections according to the following conditions  
437 in atmospheric regions: mid-tropospheric range: 1200 – 600 ppmv (Figure 6), upper tropospheric range: 600  
438 – 20 ppmv (Figure 7), and lower stratospheric range: 20 – 5 ppmv (Figure 8). This categorization is also  
439 justified by the relative influence of SEALDH-II's calculated offset uncertainty of  $\pm 3$  ppmv (Buchholz and  
440 Ebert, 2014b): At 1200 ppmv, its relative contribution of 0.25% is negligible compared to the 4.3% linear part  
441 of the uncertainty of SEALDH-II. At 5 ppmv, the relative contribution of the offset uncertainty is 60% and  
442 thus dominates the linear part of the uncertainty. Before assessing the following data, it should be  
443 emphasized again that SEALDH-II's spectroscopic first-principles evaluation was designed to rely on  
444 accurate spectral data instead of a calibration. SEALDH-II was never calibrated or referenced to any kind of  
445 reference humidity generator or sensor.

Gelöscht: Figure 6Figure 6

Gelöscht: Figure 7Figure 7

Gelöscht: Figure 8Figure 8

### 446 5.1. The 1200 – 600 ppmv range

447 Figure 6 shows the summary of the pressure dependent validations in the 1200 – 600 ppmv range. Each of  
448 the 48 data points represents the mean over one pressure measurement section of at least 60 min (see Figure  
449 4). A cubic polynomial curve fitted to the 600 ppmv results (blue) serves as an internal quasi-reference to  
450 connect with the following graphs. The 600 ppmv data (grey) are generated via a supplementary  
451 comparison at a different generator: The German national primary mid-humidity generator (PHG). This  
452 primary generator data at 600 ppmv indicate a deviation between PHG and THG of about 0.35 %, which is  
453 compatible with the uncertainties of the THG (see chapter 3.1) and the PHG (0.4%) (Buchholz et al., 2014).  
454 The PHG comparison data also allow a consistency check between the absolute values of (see Figure 2) the  
455 PHG (calibration-free), the THG (DPM calibrated) and SEALDH-II (calibration-free).

Gelöscht: Figure 6Figure 6

Gelöscht: Figure 4Figure 4

Gelöscht: Figure 2Figure 2

## 5.2. The 600 – 20 ppmv range

In this range, the linear part of the uncertainty (4.3%) and the offset uncertainty ( $\pm 3$  ppmv) have both a significant contribution. [Figure 7](#) shows a clear trend: The lower the concentration, the higher the deviation. We believe this is being caused by SEALDH-II's offset variation and will be discussed in the 20 – 5 ppmv range.

Gelöscht: Figure 7Figure 7

## 5.3. The 20 – 5 ppmv range

The results in this range ([Figure 8](#)) are dominated by the offset uncertainty. It is important to mention at this point, that the  $\pm 3$  ppmv uncertainties are calculated based on assumptions, design innovations, and several independent, synchronous measurements which are automatically done while the instrument is in operation mode (see publication (Buchholz et al., 2016; Buchholz and Ebert, 2014b)). Hence, the calculated uncertainties resemble an upper uncertainty threshold; the real deviation could be lower than 3 ppmv. A clear assessment is fairly difficult since at low concentrations (i.e., low optical densities) several other effects occur together such as, e.g., optical interference effects like fringes caused by the very long coherence length of the used laser. However, [Figure 9](#) (left) allows a rough assessment of the offset instability. This plot shows all the data below 200 ppmv, grouped by the gas pressure in the measurement cell. If one ignores the 65 hPa and 125 hPa measurements, which are clearly affected by higher order line shape effects (see above), the other measurements fit fairly well in a  $\pm 1$  ppmv envelope function (grey). In other words, SEALDH-II's combined offset "fluctuations" are below 1 ppmv H<sub>2</sub>O. All validation measurements done with SEALDH-II during the last years consistently demonstrated a small offset variability so that the observed offset error is around 0.6 ppmv — i.e., only 20% of the calculated  $\pm 3$  ppmv.

Gelöscht: Figure 8Figure 8

Gelöscht: Figure 9Figure 9

Gelöscht:

## 5.4. General evaluation

[Figure 9](#) presents a summary of all 90 analyzed concentration/pressure-pairs during the 23 days of validation. The calculated uncertainties (linear 4.3% and offset  $\pm 3$  ppmv) of SEALDH-II are plotted in purple. This uncertainty calculation doesn't include line shape deficiencies and is therefore only valid for a pressure range where the Voigt profile can be used to represent all major broadening effects of absorption lines (Dicke, 1953; Maddaloni et al., 2010). This is the case above 250 hPa. The results at 950, 750, 500, 250 hPa show that the maximum deviations, derived from these measurements, can be described by: linear +2.5%, offset -0.6 ppmv.

Gelöscht: Figure 9Figure 9

It should be noted that this result doesn't change the statement about SEALDH-II's uncertainties, since these are calculated and not based on any validation/calibration process. This is a significantly different approach between calibration-free instruments such as SEALDH-II and other classical spectroscopic instruments which rely on sensor calibration. SEALDH-II provides correctness of measurement values within its uncertainties because any effect which causes deviations has to be included in the evaluation model — otherwise it is not possible to correct for it.

Gelöscht: To prevent further interpretations, i

Gelöscht: : The holistic control/overview is one of the most important and essential differences

Gelöscht: can guarantee

As mentioned before, any calibration-free instrument can be calibrated too (see e.g. (Buchholz et al., 2013)).

509 However by doing so, one must accept to a certain extent loss of control over the system, especially in  
510 environments which are different from the calibration environment. For example, if a calibration was used  
511 to remove an instrumental offset, one has to ensure that this offset is long-term stable, which is usually  
512 quite difficult, as shown by the example of parasitic water offsets in fiber coupled diode laser hygrometers  
513 (Buchholz and Ebert, 2014b). Another option is to choose the recalibration frequency high enough; i.e.,  
514 minimizing the drift amplitude by minimizing the time between two calibrations. This, however, reduces  
515 the usable measurement time and leads to considerable investment of time and money into the calibration  
516 process. For the case of SEALDH-II, a calibration of the pressure dependence – of course tempting and easy  
517 to do – would directly “improve” SEALDH-II’s laboratory overall performance level from  $\pm 4.3\% \pm 3$  ppmv  
518 to  $\pm 0.35\% \pm 0.3$  ppmv. At first glance, this “accuracy” would then be an improvement by a factor of 55  
519 compared to the mentioned results of AquaVIT (Fahey et al., 2014). However, it is extremely difficult – if  
520 not impossible – to guarantee this performance and the validity of the calibration under harsh field  
521 conditions; instead SEALDH-II would “suffer” from the same typical calibration associated problems in  
522 stability and in predictability. Eventually, the calibration-free evaluation would define the trusted values  
523 and the “improvement”, achieved by the calibration, would have to be used very carefully and might  
524 disappear eventually.

Gelöscht:

## 525 6. Conclusion and Outlook

526 The SEALDH-II instrument, a recently developed, compact, airborne, calibration-free hygrometer  
527 (Buchholz et al., 2016) which implements a holistic, first-principle, direct, tunable diode laser absorption  
528 spectroscopy (dTDLAS) approach (Buchholz and Ebert, 2014a) was stringently validated at a traceable  
529 water vapor generator at the German national metrology institute (PTB). The pressure dependent  
530 validation covered a H<sub>2</sub>O range from 5 to 1200 ppmv and a pressure range from 65 hPa to 950 hPa. In total,  
531 90 different H<sub>2</sub>O concentration/pressure levels were studied within 23 days of permanent validation  
532 experiments. Compared to other comparisons of airborne hygrometers - such as those studied in the non-  
533 metrological AquaVIT campaign (Fahey et al., 2014), where a selection of the best “core” instruments still  
534 showed an accuracy scatter of at least  $\pm 10\%$  without an absolute reference value - our validation exercise  
535 used a traceable reference value derived from instruments directly linked to the international dew-point  
536 scale for water vapor. This allowed a direct assessment of SEALDH-II’s absolute performance with a  
537 relative accuracy level in the sub percent range. Under these conditions, SEALDH-II showed an excellent  
538 absolute agreement within its uncertainties which are 4.3% of the measured value plus an offset of  $\pm 3$  ppmv  
539 (valid at 1013 hPa). SEALDH-II showed at lower gas pressures - as expected - a stable, systematic, pressure  
540 dependent offset to the traceable reference, which is caused by the line shape deficiencies of the Voigt line  
541 shape: e.g. at 950 hPa, the systematic deviation of the calibration-free evaluated results could be described  
542 by (linear +0.9%, offset -0.5 ppmv), while at 250 hPa the systematic deviations could be described by (linear  
543 +2.5%, offset -0.6 ppmv). If we suppress this systematic pressure dependence, the purely statistical  
544 deviation is described by linear scatter of  $\pm 0.35\%$  and an offset uncertainty of  $\pm 0.3$  ppmv.

Gelöscht: ;

Gelöscht: novel

Gelöscht: s

Gelöscht: tly

Gelöscht: tuneable

551 Due to its extensive internal monitoring and correction infrastructure, SEALDH-II is very resilient against a  
 552 broad range of external disturbances and has an output signal temperature coefficient of only 0.026%/K,  
 553 which has already been validated earlier (Buchholz et al., 2016). Therefore, these results can be directly  
 554 transferred into harsh field environments. With this metrological validation presented here, SEALDH-II is  
 555 the first directly deployable, metrologically validated, airborne transfer standard for atmospheric water  
 556 vapor. Having already been deployed in several airborne and laboratory measurement campaigns,  
 557 SEALDH-II thus directly links for the first time, scientific campaign results to the international metrological  
 558 water vapor scale. \_\_\_\_\_

Gelöscht: , mid and upper atmosphere  
 focused  
 Gelöscht: we believe  
 Gelöscht: to be  
 Gelöscht: .

559 For future applications, the measurement path length of 1.5 m and hence SEALDH-II's sensitivity could be  
 560 relatively quickly enhanced by a factor of 5-10 by implementing a longer path absorption cell. A linear  
 561 increase of the absorption path yield a proportional scaling of the SEALDH-II's dynamic range (currently at  
 562 1.5 m: 3 – 40 000 ppmv; lower limit defined by the calculated offset uncertainty of  $\pm 3$  ppmv). With this  
 563 fairly simple adaption SEALDH-II could be adapted to lower H<sub>2</sub>O concentration ranges, which would make  
 564 SEALDH-II more suitable for stratospheric applications. The calculated offset uncertainty of SEALDH-II is  
 565 reciprocally correlated the optical path-length. Therefore, an increase of the current 1.5 m optical path  
 566 length to e.g. 30 m or more with different cell designs such as (McManus et al., 1995) or (Tuzson et al., 2013),  
 567 would allow to reduce the offset uncertainty to 0.15 ppmv; the above discussed laboratory offset deviation  
 568 performance could reach levels of down to  $\pm 0.015$  ppmv.

Gelöscht: T  
 Gelöscht: he  
 Gelöscht: range of  
 Gelöscht:  
 Gelöscht:  
 Gelöscht: to be  
 Gelöscht: conditions  
 Gelöscht: a other  
 Gelöscht: s  
 Gelöscht: , or XXX  
 Gelöscht: suppress  
 Gelöscht: ;  
 Gelöscht: and

#### 570 **Data availability**

571 *The underlying data for the results shown in this paper are raw spectra (time vs. photo current), which are compressed*  
 572 *to be compatible with the instruments data storage. In the compressed state the total amount is approximately 6GB of*  
 573 *binary data. Uncompressed data size is approx. 60 GB. We are happy to share these data on request.*

#### 575 **Author Contributions**

576 *Bernhard Buchholz and Volker Ebert conceived and designed the experiments. Bernhard Buchholz performed the*  
 577 *experiments; Bernhard Buchholz and Volker Ebert analyzed the data and wrote the paper.*

#### 579 **Conflicts of Interest**

580 *The authors declare no conflict of interest*

#### 582 **Acknowledgements:**

583 *Parts of this work were embedded in the EMPIR (European Metrology Program for Innovation and Research) projects*  
 584 *METEOMET- 1 and METEOMET-2. The authors want to thank Norbert Böse and Sonja Pratzler (PTB Germany)*  
 585 *for operating the German primary national water standard and the traceable humidity generator. Last but not least,*  
 586 *the authors thank James McSpiritt (Princeton University) for the various discussions about reliable sensor designs*  
 587 *and Mark Zondlo (Princeton University) for sharing his broad knowledge about atmospheric water vapor*  
 588 *measurements.*





## 608 7. References

- 609 Buchholz, B., Afchine, A., Klein, A., Schiller, C. and Krämer, M.: HAI , a new airborne, absolute, twin dual-  
610 channel, multi-phase TDLAS-hygrometer: background, design, setup, and first flight data, *Atmos. Meas.*  
611 *Tech.*, 5194, DOI: 10.5194/amt-10-35-2017, <http://dx.doi.org/10.5194/amt-10-35-2017>, 2017.
- 612 Buchholz, B., Böse, N. and Ebert, V.: Absolute validation of a diode laser hygrometer via intercomparison  
613 with the German national primary water vapor standard, *Applied Physics B*, 116(4), 883–899, DOI:  
614 10.1007/s00340-014-5775-4, <http://dx.doi.org/10.1007/s00340-014-5775-4>, 2014.
- 615 Buchholz, B. and Ebert, V.: Holistic TDLAS spectrometry: The role of comprehensive housekeeping data for  
616 robust quality assurance illustrated by two absolute, airborne TDLAS Hygrometers: SEALDH-II and HAI,  
617 FLAIR 2014 - Field Laser Applications in Industry and Research, 2014a.
- 618 Buchholz, B. and Ebert, V.: Offsets in fiber-coupled diode laser hygrometers caused by parasitic absorption  
619 effects and their prevention, *Measurement Science and Technology*, 25(7), 75501, DOI: 10.1088/0957-  
620 0233/25/7/075501, <http://dx.doi.org/10.1088/0957-0233/25/7/075501>, 2014b.
- 621 Buchholz, B., Kallweit, S. and Ebert, V.: SEALDH-II—An Autonomous, Holistically Controlled, First  
622 Principles TDLAS Hygrometer for Field and Airborne Applications: Design–Setup–Accuracy/Stability  
623 Stress Test, *Sensors*, 17(1), 68, DOI: 10.3390/s17010068, <http://dx.doi.org/10.3390/s17010068>, 2016.
- 624 Buchholz, B., Kühnreich, B., Smit, H. G. J. and Ebert, V.: Validation of an extractive, airborne, compact TDL  
625 spectrometer for atmospheric humidity sensing by blind intercomparison, *Applied Physics B*, 110(2), 249–  
626 262, DOI: 10.1007/s00340-012-5143-1, <http://dx.doi.org/10.1007/s00340-012-5143-1>, 2013.
- 627 Buck, A.: The Lyman-alpha absorption hygrometer, in *Moisture and Humidity Symposium Washington*,  
628 DC, Research Triangle Park, NC, pp. 411–436., 1985.
- 629 Busen, R. and Buck, A. L.: A High-Performance Hygrometer for Aircraft Use: Description, Installation, and  
630 Flight Data, *Journal of Atmospheric and Oceanic Technology*, 12, 73–84, DOI: 10.1175/1520-  
631 0426(1995)012<0073:AHPHFA>2.0.CO;2, [http://dx.doi.org/10.1175/1520-0426\(1995\)012<0073:AHPHFA>2.0.CO;2](http://dx.doi.org/10.1175/1520-0426(1995)012<0073:AHPHFA>2.0.CO;2), 1995.
- 633 Cerni, T. A.: An Infrared Hygrometer for Atmospheric Research and Routine Monitoring, *Journal of*  
634 *Atmospheric and Oceanic Technology*, 11, 445–462, DOI: 10.1175/1520-  
635 0426(1994)011<0445:AIHFAR>2.0.CO;2, [http://dx.doi.org/10.1175/1520-0426\(1994\)011<0445:AIHFAR>2.0.CO;2](http://dx.doi.org/10.1175/1520-0426(1994)011<0445:AIHFAR>2.0.CO;2), 1994.
- 637 Desjardins, R., MacPherson, J., Schuepp, P. and Karanja, F.: An evaluation of aircraft flux measurements of  
638 CO<sub>2</sub>, water vapor and sensible heat, *Boundary-Layer Meteorology*, 47(1), 55–69, DOI: 10.1007/BF00122322,  
639 <http://dx.doi.org/10.1007/BF00122322>, 1989.
- 640 Dicke, R.: The effect of collisions upon the Doppler width of spectral lines, *Physical Review*, 89(2), 472–473,  
641 DOI: 10.1103/PhysRev.89.472, <http://dx.doi.org/10.1103/PhysRev.89.472>, 1953.
- 642 Diskin, G. S., Podolske, J. R., Sachse, G. W. and Slate, T. A.: Open-path airborne tunable diode laser  
643 hygrometer, in *Proc. SPIE 4817, Diode Lasers and Applications in Atmospheric Sensing*, vol. 4817, pp. 196–  
644 204., 2002.
- 645 Durry, G., Amarouche, N., Joly, L. and Liu, X.: Laser diode spectroscopy of H<sub>2</sub>O at 2.63  $\mu$ m for atmospheric  
646 applications, *Applied Physics B*, 90(3–4), 573–580, DOI: 10.1007/s00340-007-2884-3,  
647 <http://dx.doi.org/10.1007/s00340-007-2884-3>, 2008.
- 648 Ebert, V., Fernholz, T. and Pitz, H.: In-situ monitoring of water vapour and gas temperature in a coal fired  
649 power-plant using near-infrared diode lasers, in *Laser Applications to Chemical and Environmental*  
650 *Analysis*, pp. 4–6, Optical Society of America. [online] Available from:  
651 <http://www.opticsinfobase.org/abstract.cfm?id=142068> (Accessed 15 February 2012), 2000.
- 652 Ebert, V. and Wolfrum, J.: Absorption spectroscopy, in *OPTICAL MEASUREMENTS-Techniques and*  
653 *Applications*, ed. F. Mayinger, pp. 273–312, Springer., 1994.

654 Fahey, D. W., Saathoff, H., Schiller, C., Ebert, V., Peter, T., Amarouche, N., Avallone, L. M., Bauer, R.,  
 655 Christensen, L. E., Durr, G., Dyroff, C., Herman, R., Hunsmann, S., Khaykin, S., Mackrodt, P., Smith, J. B.,  
 656 Spelten, N., Troy, R. F., Wagner, S. and Wienhold, F. G.: The AquaVIT-1 intercomparison of atmospheric  
 657 water vapor measurement techniques, *Atmospheric Measurement Techniques*, 7, 3159–3251, DOI:  
 658 10.5194/amtd-7-3159-2014, <http://dx.doi.org/10.5194/amtd-7-3159-2014>, 2014.

659 Gurlit, W., Zimmermann, R., Giesemann, C., Fernholz, T., Ebert, V., Wolfrum, J., Platt, U. U. and Burrows, J.  
 660 P.: Lightweight diode laser spectrometer “CHILD” for balloon-borne measurements of water vapor and  
 661 methane, *Applied Optics*, 44(1), 91–102, DOI: 10.1364/AO.44.000091,  
 662 <http://dx.doi.org/10.1364/AO.44.000091>, 2005.

663 Hansford, G. M., Freshwater, R. A., Eden, L., Turnbull, K. F. V., Hadaway, D. E., Ostanin, V. P. and Jones, R.  
 664 L.: Lightweight dew-/frost-point hygrometer based on a surface-acoustic-wave sensor for balloon-borne  
 665 atmospheric water vapor profile sounding, *Review of scientific instruments*, 77, 014502–014502, DOI:  
 666 10.1063/1.2140275, <http://dx.doi.org/10.1063/1.2140275>, 2006.

667 Heinonen, M., Anagnostou, M., Bell, S., Stevens, M., Benyon, R., Bergerud, R. A., Bojkovski, J., Bosma, R.,  
 668 Nielsen, J., Böse, N., Cromwell, P., Kartal Dogan, A., Aytekin, S., Uytun, A., Fernicola, V., Flakiewicz, K.,  
 669 Blanquart, B., Hudoklin, D., Jacobson, P., Kentved, A., Lóio, I., Mamontov, G., Masarykova, A., Mitter, H.,  
 670 Mnguni, R., Otych, J., Steiner, A., Szilágyi Zsófia, N. and Zvizdic, D.: Investigation of the equivalence of  
 671 national dew-point temperature realizations in the -50 °C to +20 °C range, *International Journal of*  
 672 *Thermophysics*, 33(8–9), 1422–1437, DOI: 10.1007/s10765-011-0950-x, [http://dx.doi.org/10.1007/s10765-011-](http://dx.doi.org/10.1007/s10765-011-0950-x)  
 673 [0950-x](http://dx.doi.org/10.1007/s10765-011-0950-x), 2012.

674 Held, I. and Soden, B.: Water vapor feedback and global warming, *Annual review of energy and the*  
 675 *environment*, 25(1), 441–475, DOI: 10.1146/annurev.energy.25.1.441,  
 676 <http://dx.doi.org/10.1146/annurev.energy.25.1.441>, 2000.

677 Helten, M., Smit, H. G. J., Sträter, W., Kley, D., Nedelec, P., Zöger, M. and Busen, R.: Calibration and  
 678 performance of automatic compact instrumentation for the measurement of relative humidity from  
 679 passenger aircraft, *Journal of Geophysical Research: Atmospheres*, 103(D19), 25643–25652, DOI:  
 680 10.1029/98JD00536, <http://dx.doi.org/10.1029/98JD00536>, 1998.

681 Houghton, J.: *Global warming: The complete briefing*, Cambridge University Press. [online] Available from:  
 682 <http://britastro.org/jbaa/pdf/114-6shanklin.pdf> (Accessed 14 May 2014), 2009.

683 Hunsmann, S., Wunderle, K., Wagner, S., Rascher, U., Schurr, U. and Ebert, V.: Absolute, high resolution  
 684 water transpiration rate measurements on single plant leaves via tunable diode laser absorption  
 685 spectroscopy (TDLAS) at 1.37  $\mu\text{m}$ , *Applied Physics B*, 92(3), 393–401, DOI: 10.1007/s00340-008-3095-2,  
 686 <http://dx.doi.org/10.1007/s00340-008-3095-2>, 2008.

687 JCGM 2008: JCGM 200 : 2008 International vocabulary of metrology — Basic and general concepts and  
 688 associated terms ( VIM ) Vocabulaire international de métrologie — Concepts fondamentaux et généraux et  
 689 termes associés ( VIM ), International Organization for Standardization, 3(Vim), 104, DOI: 10.1016/0263-  
 690 2241(85)90006-5, [http://dx.doi.org/10.1016/0263-2241\(85\)90006-5](http://dx.doi.org/10.1016/0263-2241(85)90006-5), 2008.

691 Joint Committee for Guides in Metrology (JCGM): Evaluation of measurement data - An introduction to the  
 692 “Guide to the expression of uncertainty in measurement” and related documents, BIPM: Bureau  
 693 International des Poids et Mesures, [www.bipm.org](http://www.bipm.org), 2009.

694 Karpechko, A. Y., Perlwitz, J. and Manzini, E.: *Journal of Geophysical Research : Atmospheres*, , 1–16, DOI:  
 695 10.1002/2013JD021350, <http://dx.doi.org/10.1002/2013JD021350>, 2014.

696 Kiehl, J. T. and Trenberth, K. E.: Earth’s Annual Global Mean Energy Budget, *Bulletin of the American*  
 697 *Meteorological Society*, 78(2), 197–208, DOI: 10.1175/1520-0477(1997)078<0197:EAGMEB>2.0.CO;2,  
 698 [http://dx.doi.org/10.1175/1520-0477\(1997\)078<0197:EAGMEB>2.0.CO;2](http://dx.doi.org/10.1175/1520-0477(1997)078<0197:EAGMEB>2.0.CO;2), 1997.

699 Kley, D. and Stone, E.: Measurement of water vapor in the stratosphere by photodissociation with Ly  $\alpha$   
 700 (1216 Å) light, *Review of Scientific Instruments*, 49(6), 691, DOI: 10.1063/1.1135596,  
 701 <http://dx.doi.org/10.1063/1.1135596>, 1978.

Krämer, M., Schiller, C., Afchine, A., Bauer, R., Gensch, I., Mangold, A., Schlicht, S., Spelten, N., Sitnikov, N., Borrmann, S., Reus, M. de and Spichtinger, P.: Ice supersaturations and cirrus cloud crystal numbers, *Atmospheric and Oceanic Optics*, 9, 3505–3522, DOI: 10.5194/acp-9-3505-2009, <http://dx.doi.org/10.5194/acp-9-3505-2009>, 2009.

Kühnreich, B., Höh, M., Wagner, S. and Ebert, V.: Direct single-mode fibre-coupled miniature White cell for laser absorption spectroscopy, *Review of Scientific Instruments*, 87(2), 0–8, DOI: 10.1063/1.4941748, <http://dx.doi.org/10.1063/1.4941748>, 2016.

Ludlam, F.: Clouds and storms: The behavior and effect of water in the atmosphere. [online] Available from: <http://agris.fao.org/agris-search/search.do?recordID=US8025686> (Accessed 24 May 2014), 1980.

Mackrodt, P.: A New Attempt on a Coulometric Trace Humidity Generator, *International Journal of Thermophysics*, 33(8–9), 1520–1535, DOI: 10.1007/s10765-012-1348-0, <http://dx.doi.org/10.1007/s10765-012-1348-0>, 2012.

Maddaloni, P., Malara, P. and Natale, P. De: Simulation of Dicke-narrowed molecular spectra recorded by off-axis high-finesse optical cavities, *Molecular Physics*, 108(6), 749–755, DOI: 10.1080/00268971003601571, <http://dx.doi.org/10.1080/00268971003601571>, 2010.

May, R. D.: Open-path, near-infrared tunable diode laser spectrometer for atmospheric measurements of H<sub>2</sub>O, *Journal of Geophysical Research*, 103(D15), 19161–19172, DOI: 10.1029/98JD01678, <http://dx.doi.org/10.1029/98JD01678>, 1998.

Maycock, A. C., Shine, K. P. and Joshi, M. M.: The temperature response to stratospheric water vapour changes, *Quarterly Journal of the Royal Meteorological Society*, 137, 1070–1082, DOI: 10.1002/qj.822, <http://dx.doi.org/10.1002/qj.822>, 2011.

MBW Calibration Ltd.: MBW 373HX, 2010.

McManus, J., Keabian, P. and Zahniser, M.: Astigmatic mirror multipass absorption cells for long-path-length spectroscopy, *Applied Optics*, 34(18), 3336–3348, DOI: 10.1364/AO.34.003336, <http://dx.doi.org/10.1364/AO.34.003336>, 1995.

Meyer, J., Rolf, C., Schiller, C., Rohs, S., Spelten, N., Afchine, A., Zöger, M., Sitnikov, N., Thornberry, T. D., Rollins, A. W., Bozoki, Z., Tatrai, D., Ebert, V., Kühnreich, B., Mackrodt, P., Möhler, O., Saathoff, H., Rosenlof, K. H. and Krämer, M.: Two decades of water vapor measurements with the FISH fluorescence hygrometer: A review, *Atmospheric Chemistry and Physics*, 15(14), 8521–8538, DOI: 10.5194/acp-15-8521-2015, <http://dx.doi.org/10.5194/acp-15-8521-2015>, 2015.

Möller, D., Feichter, J. and Herrmann, H.: Von Wolken, Nebel und Niederschlag, in *Chemie über den Wolken... und darunter*, edited by R. Zellner, pp. 236–240, WILEY-VCH Verlag GmbH & Co. KGaA, Weinheim, 2011.

Muecke, R. J., Scheumann, B., Slemr, F. and Werle, P. W.: Calibration procedures for tunable diode laser spectrometers, *Proc. SPIE 2112, Tunable Diode Laser Spectroscopy, Lidar, and DIAL Techniques for Environmental and Industrial Measurement*, 2112, 87–98, DOI: 10.1117/12.177289, <http://dx.doi.org/10.1117/12.177289>, 1994.

Ohtaki, E. and Matsui, T.: Infrared device for simultaneous measurement of fluctuations of atmospheric carbon dioxide and water vapor, *Boundary-Layer Meteorology*, 24(1), 109–119, DOI: 10.1007/BF00121803, <http://dx.doi.org/10.1007/BF00121803>, 1982.

Peter, T., Marcolli, C., Spichtinger, P., Corti, T., Baker, M. B. and Koop, T.: When dry air is too humid, *Science*, 314(5804), 1399–1402, DOI: 10.1126/science.1135199, <http://dx.doi.org/10.1126/science.1135199>, 2006.

Petersen, R., Cronce, L., Feltz, W., Olson, E. and Helms, D.: WVSS-II moisture observations: A tool for validating and monitoring satellite moisture data, *EUMETSAT Meteorological Satellite Conference*, 22, 67–77 [online] Available from: [http://www.eumetsat.int/Home/Main/AboutEUMETSAT/Publications/ConferenceandWorkshopProceedings/2010/groups/cps/documents/document/pdf\\_conf\\_p57\\_s1\\_03\\_petersen\\_v.pdf](http://www.eumetsat.int/Home/Main/AboutEUMETSAT/Publications/ConferenceandWorkshopProceedings/2010/groups/cps/documents/document/pdf_conf_p57_s1_03_petersen_v.pdf) (Accessed 20 February 2017), 2010.

750 Ravishankara, A. R.: Water Vapor in the Lower Stratosphere, *Science*, 337(6096), 809–810, DOI:  
751 10.1126/science.1227004, <http://dx.doi.org/10.1126/science.1227004>, 2012.

752 Rollins, A., Thornberry, T., Gao, R. S., Smith, J. B., Sayres, D. S., Sargent, M. R., Schiller, C., Krämer, M.,  
753 Spelten, N., Hurst, D. F., Jordan, A. F., Hall, E. G., Vömel, H., Diskin, G. S., Podolske, J. R., Christensen, L.  
754 E., Rosenlof, K. H., Jensen, E. J. and Fahey, D. W.: Evaluation of UT/LS hygrometer accuracy by  
755 intercomparison during the NASA MACPEX mission, *Journal of Geophysical Research: Atmospheres*, 119,  
756 DOI: 10.1002/2013JD020817, <http://dx.doi.org/10.1002/2013JD020817>, 2014.

757 Roths, J. and Busen, R.: Development of a laser in situ airborne hygrometer (LISAH) (feasibility study),  
758 *Infrared physics & technology*, 37(1), 33–38, DOI: 10.1016/1350-4495(95)00103-4,  
759 [http://dx.doi.org/10.1016/1350-4495\(95\)00103-4](http://dx.doi.org/10.1016/1350-4495(95)00103-4), 1996.

760 Salasmaa, E. and Kostamo, P.: HUMICAP® thin film humidity sensor, in *Advanced Agricultural*  
761 *Instrumentation Series E: Applied Sciences*, edited by W. G. Gensler, pp. 135–147, Kluwer., 1986.

762 Scherer, M., Vömel, H., Fueglistaler, S., Oltmans, S. J. and Staehelin, J.: Trends and variability of midlatitude  
763 stratospheric water vapour deduced from the re-evaluated Boulder balloon series and HALOE,  
764 *Atmospheric Chemistry and Physics*, 8, 1391–1402, DOI: 10.5194/acp-8-1391-2008,  
765 <http://dx.doi.org/10.5194/acp-8-1391-2008>, 2008.

766 Schiff, H. I., Mackay, G. I. and Bechara, J.: The use of tunable diode laser absorption spectroscopy for  
767 atmospheric measurements, *Research on Chemical Intermediates*, 20(3), 525–556, DOI:  
768 10.1163/156856794X00441, <http://dx.doi.org/10.1163/156856794X00441>, 1994.

769 Schulz, C., Dreizler, A., Ebert, V. and Wolfrum, J.: Combustion Diagnostics, in *Handbook of Experimental*  
770 *Fluid Mechanics*, edited by C. Tropea, A. L. Yarin, and J. F. Foss, pp. 1241–1316, Springer Berlin Heidelberg,  
771 Heidelberg., 2007.

772 Sherwood, S., Bony, S. and Dufresne, J.: Spread in model climate sensitivity traced to atmospheric  
773 convective mixing, *Nature*, 505(7481), 37–42, DOI: 10.1038/nature12829,  
774 <http://dx.doi.org/10.1038/nature12829>, 2014.

775 Silver, J. A. and Hovde, D. C.: Near-infrared diode laser airborne hygrometer, *Review of scientific*  
776 *instruments*, 65(5), 1691–1694, DOI: 10.1063/1.1144861, <http://dx.doi.org/10.1063/1.1144861>, 1994a.

777 Silver, J. and Hovde, D.: Near-infrared diode laser airborne hygrometer, *Review of scientific instruments*,  
778 65, 5, 1691–1694 [online] Available from: [http://ieeexplore.ieee.org/xpls/abs\\_all.jsp?arnumber=4991817](http://ieeexplore.ieee.org/xpls/abs_all.jsp?arnumber=4991817)  
779 (Accessed 25 November 2013b), 1994.

780 Smit, H. G. J., Rolf, C., Kraemer, M., Petzold, A., Spelten, N., Neis, P., Maser, R., Buchholz, B., Ebert, V. and  
781 Tatrai, D.: Development and Evaluation of Novel and Compact Hygrometer for Airborne Research  
782 (DENCHAR): In-Flight Performance During AIRTOSS-I / II Research Aircraft Campaigns, *Geophysical*  
783 *Research Abstracts*, 16(EGU2014-9420), 2014.

784 Sonntag, D.: Important new Values of the Physical Constants of 1968, Vapour Pressure Formulations based  
785 on the ITS-90, and Psychrometer Formulae, *Meteorologische Zeitschrift*, 40(5), 340–344, 1990.

786 Thornberry, T. D., Rollins, A. W., Gao, R. S., Watts, L. A., Ciciora, S. J., McLaughlin, R. J. and Fahey, D. W.:  
787 A two-channel, tunable diode laser-based hygrometer for measurement of water vapor and cirrus cloud ice  
788 water content in the upper troposphere and lower stratosphere, *Atmospheric Measurement Techniques*  
789 *Discussions*, 7(8), 8271–8309, DOI: 10.5194/amtd-7-8271-2014, <http://dx.doi.org/10.5194/amtd-7-8271-2014>,  
790 2014.

791 Thunder-Scientific: Model 2500 Two-Pressure Humidity Generator, [online] Available from:  
792 [www.thunderscientific.com](http://www.thunderscientific.com) (Accessed 12 May 2016), 2016.

793 Tuzson, B., Mangold, M., Looser, H., Manninen, A. and Emmenegger, L.: Compact multipass optical cell for  
794 laser spectroscopy., *Optics letters*, 38(3), 257–9, DOI: 10.1364/OL.38.000257,  
795 <http://dx.doi.org/10.1364/OL.38.000257>, 2013.

796 Webster, C., Flesch, G., Mansour, K., Haberle, R. and Bauman, J.: Mars laser hygrometer, *Applied optics*,  
797 43(22), 4436–4445, DOI: 10.1364/AO.43.004436, <http://dx.doi.org/10.1364/AO.43.004436>, 2004.

798 White, J.: Very long optical paths in air, *Journal of the Optical Society of America* (1917-1983), 66(5), 411–  
799 416, DOI: 10.1364/JOSA.66.000411, <http://dx.doi.org/10.1364/JOSA.66.000411>, 1976.

800 Wiederhold, P. R.: *Water Vapor Measurement. Methods and Instrumentation*, Har/Dskt., CRC Press., 1997.

801 Zöger, M., Afchine, A., Eicke, N., Gerhards, M.-T., Klein, E., McKenna, D. S., Mörschel, U., Schmidt, U., Tan,  
802 V., Tuitjer, F., Woyke, T. and Schiller, C.: Fast in situ stratospheric hygrometers: A new family of balloon-  
803 borne and airborne Lyman photofragment fluorescence hygrometers, *Journal of Geophysical Research*,  
804 104(D1), 1807–1816, DOI: 10.1029/1998JD100025, <http://dx.doi.org/10.1029/1998JD100025>, 1999a.

805 Zöger, M., Engel, A., McKenna, D. S., Schiller, C., Schmidt, U. and Woyke, T.: Balloon-borne in situ  
806 measurements of stratospheric H<sub>2</sub>O, CH<sub>4</sub> and H<sub>2</sub> at midlatitudes, *Journal of Geophysical Research*,  
807 104(D1), 1817–1825, DOI: 10.1029/1998JD100024, <http://dx.doi.org/10.1029/1998JD100024>, 1999b.

808

809

# **Figures:**

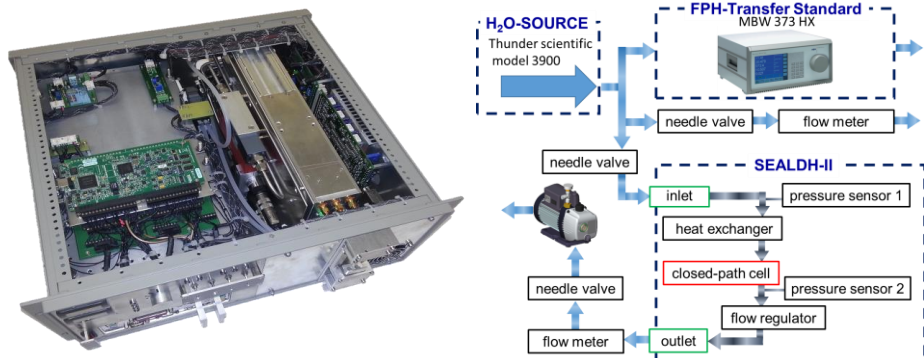


Figure 1: Left: Photo of SEALDH-II, the Selective Extractive Airborne Laser Diode Hygrometer (dimension 19" 4 U). Right: Setup for the metrological absolute accuracy validation. The combination of a H<sub>2</sub>O source together with a traceable dew point hygrometer, DPM, is used as a transfer standard – a traceable humidity generator (THG).

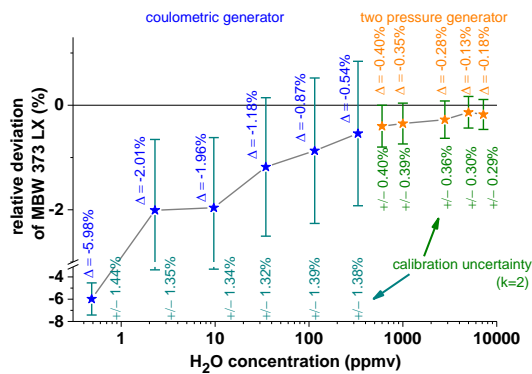


Figure 2: Calibration of the DPM (dew/frost point mirror hygrometer, MBW 373 LX, which is used as part of the THG) at the national primary water vapor standards of Germany. The standard for the higher H<sub>2</sub>O concentration range (orange) is a "two pressure generator" (Buchholz et al., 2014); for the lower concentration range (blue) a "coulometric generator" (Mackrodt, 2012) is used as a reference. The deviations between reference and DPM are labelled with "Δ". The uncertainties of every individual calibration point are stated as green numbers below every single measurement point.

Gelöscht:

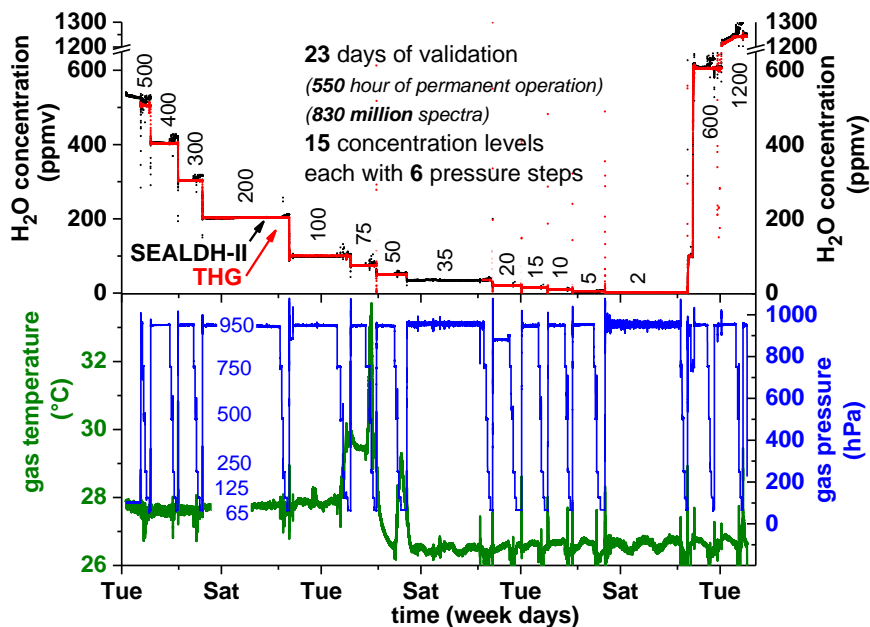


Figure 3: Overview showing all data recorded over 23 days of validation experiments. Measurements of the traceable humidity generator (THG) are shown in red, SEALDH-II data in black, gas pressure and gas temperature in SEALDH-II's measurement cell are shown in blue and green. Note: SEALDH-II operated the entire time without any malfunctions; the THG didn't save data in the 35 ppmv section; the temperature increase during the 75 ppmv section was caused by a defect of the air conditioning in the laboratory.

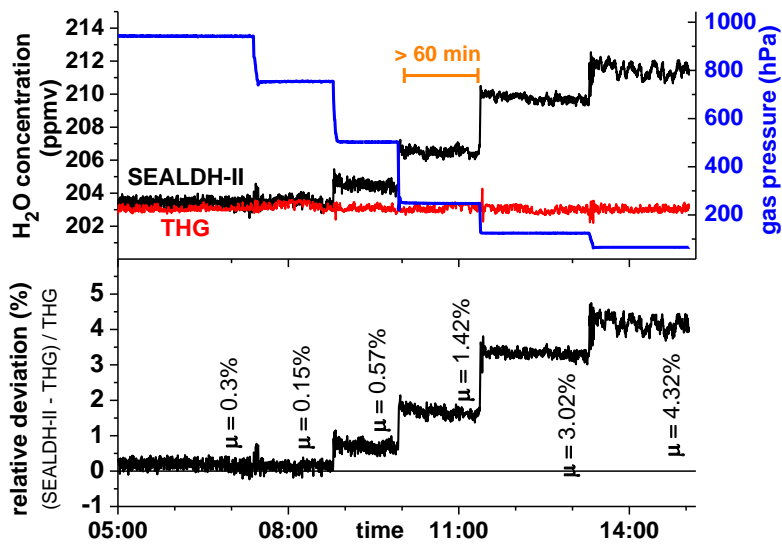


Figure 4: Detailed plot of the validation at 200 ppmv with six gas pressure steps from 50 to 950 hPa. Each individual pressure level was maintained for at least 60 minutes in order to avoid any dynamic or hysteresis effects and to facilitate clear accuracy assessments. The  $\mu$ -values define the averaged relative deviation on every gas pressure level.

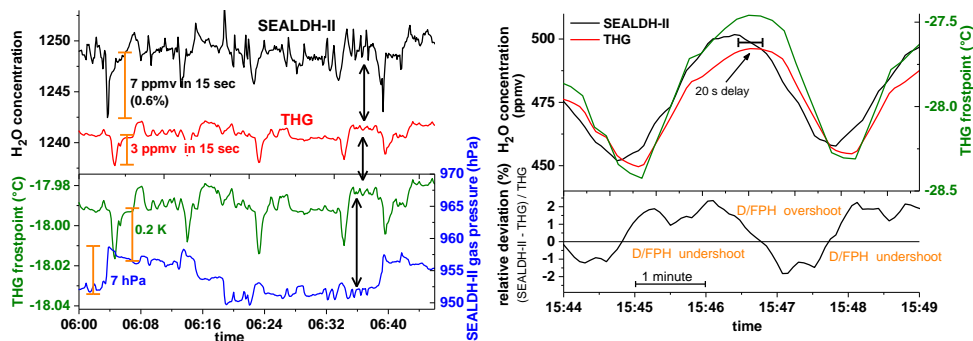


Figure 5: Short term  $H_2O$  fluctuations in the generated water vapor flow measured by SEALDH-II and the dew/frost point mirror hygrometer (D/FPH) of the traceable humidity generator (THG). The different dynamic characteristics of SEALDH-II (fast response time) and THG (quite slow response) lead in a direct comparison to artificial noise. Oscillating behaviors like in the right figure occur when the THG is not equilibrated. We did not use such data segments for the accuracy assessments.

Gelöscht:



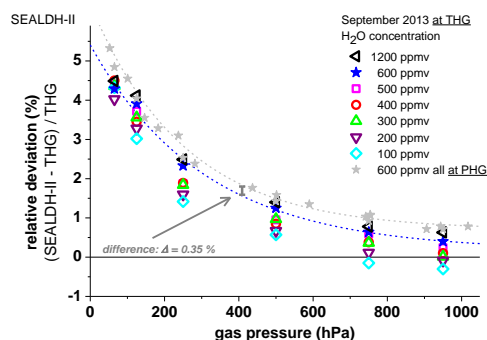


Figure 6: Gas pressure dependent comparison between SEALDH-II and THG over a H<sub>2</sub>O concentration range from 600 to 1200 ppmv and a pressure range from 50 to 950 hPa. The 600 ppmv values (in grey) are measured directly at the national primary humidity generator (PHG) of Germany; all other H<sub>2</sub>O concentration values are measured at and compared to the traceable humidity generator (THG). All SEALDH-II spectra were evaluated with a calibration-free first principles evaluation based on absolute spectral parameters. No initial or repetitive calibration of SEALDH-II with respect to any “water reference” source was used.

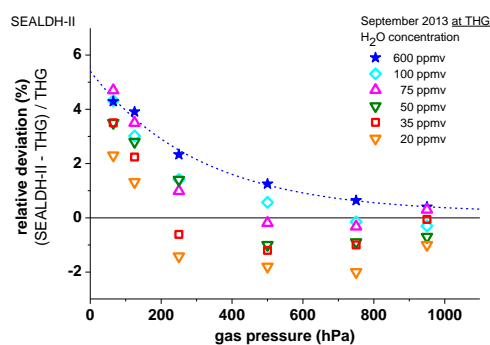
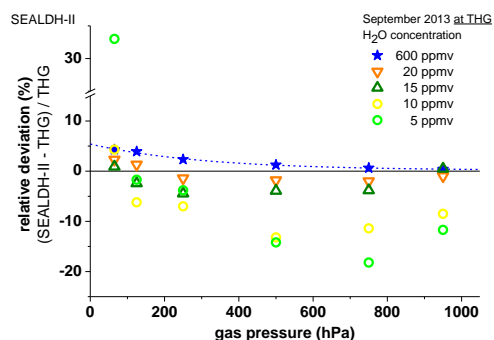


Figure 7: Comparison results as in Figure 6 but for the 200 – 600 ppmv range.

Gelöscht: Figure 6Figure 6



874 | Figure 8: Comparison results as in [Figure 6](#) and [Figure 7](#) but for the 5 – 20 ppmv range. All spectra are determined with  
875 a calibration-free first principles evaluation concept. The major contribution to the higher fluctuations at lower  
876 concentrations is the accuracy of the offset determination (details see text).

Gelöscht: Figure 6Figure 6

Gelöscht: Figure 7Figure 7

877

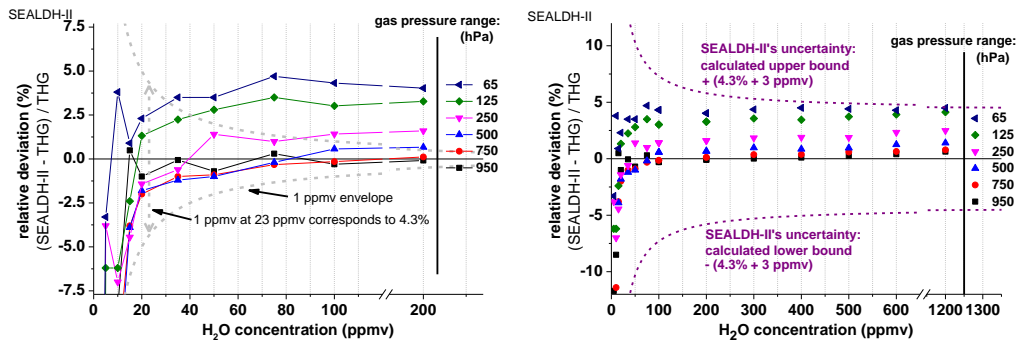


Figure 9: Direct comparison of SEALDH-II versus THG for H<sub>2</sub>O concentrations between 5 and 200 ppmv and gas pressures from 65 to 950 hPa. Both figures show the relative deviations between SEALDH-II and THG grouped and color-coded by gas-pressure. Left plot: relative deviations of SEALDH-II versus THG below 200 ppmv; the grey line indicates the computed relative effect in SEALDH-II's performance caused by  $\pm 1$  ppmv offset fluctuation. This line facilitates a visual comparison between an offset impact and the 4.3% linear part of the uncertainty of SEALDH-II. Right plot: relative deviations for all measured data in the same concentration range. Also shown is SEALDH-II's total uncertainty of  $4.3\% \pm 3$  ppmv (calculated for 1013 hPa) as a dashed line.

878

879

880